PROCEEDINGS OF THE ROYAL SOCIETY A MATHEMATICAL, PHYSICAL & ENGINEERING SCIENCES

Experimental evidence for the role of ions in particle nucleation under atmospheric conditions

Henrik Svensmark, Jens Olaf P Pedersen, Nigel D Marsh, Martin B Enghoff and Ulrik I Uggerhøj

Proc. R. Soc. A 2007 **463**, 385-396
doi: 10.1098/rspa.2006.1773

PROCEEDINGS OF THE ROYAL SOCIETY A

Proc. R. Soc. A (2007) **463**, 385–396
doi:10.1098/rspa.2006.1773
Published online 3 October 2006

Experimental evidence for the role of ions in particle nucleation under atmospheric conditions

By Henrik Svensmark[1,*], Jens Olaf P. Pedersen[1], Nigel D. Marsh[1], Martin B. Enghoff[1] and Ulrik I. Uggerhøj[1,2]

[1]*Centre for Sun-Climate Research, Danish National Space Centre, 2100 Copenhagen, Denmark*
[2]*Institute of Physics and Astronomy, University of Aarhus, 8000 Aarhus, Denmark*

Experimental studies of aerosol nucleation in air, containing trace amounts of ozone, sulphur dioxide and water vapour at concentrations relevant for the Earth's atmosphere, are reported. The production of new aerosol particles is found to be proportional to the negative ion density and yields nucleation rates of the order of 0.1–1 $\mathrm{cm}^{-3}\,\mathrm{s}^{-1}$. This suggests that the ions are active in generating an atmospheric reservoir of small thermodynamically stable clusters, which are important for nucleation processes in the atmosphere and ultimately for cloud formation.

Keywords: cosmic rays; aerosol nucleation; clouds

1. Introduction

The role of ions in the production of aerosols is among the least understood, but potentially is an important, process in the Earth's atmosphere. Atmospheric (Hoppel *et al.* 1994; Clarke *et al.* 1998; Birmili *et al.* 2003; Lee *et al.* 2003; Kulmala *et al.* 2004) and experimental (Berndt *et al.* 2005) observations have shown that the nucleation of aerosol particles can occur under conditions that cannot be explained by classical nucleation theory. Several ideas have been put forward to solve this nucleation problem, e.g. ion-induced nucleation (Arnold 1980; Raes *et al.* 1986; Turco *et al.* 1998) and ternary nucleation (Kulmala *et al.* 2000). However, experimental investigations exploring the role of ions in particle production are scarce and often at conditions far removed from those relevant for the lower part of the atmosphere (Bricard *et al.* 1968; Vohra *et al.* 1984; Kim *et al.* 2002; Nagato *et al.* 2005; Wilhelm *et al.* 2003). Here, we show that the production of new aerosol particles is proportional to the negative ion density under experimental conditions similar to those found in the lower troposphere over oceans. Since production rates at 3 nm were observed to be 1–10 $\mathrm{cm}^{-3}\,\mathrm{s}^{-1}$, and numerical simulations yielded nucleation rates of initial stable clusters (approx. 1 nm) around 0.1–1 $\mathrm{cm}^{-3}\,\mathrm{s}^{-1}$, it is suggested that ions

* Author for correspondence (hsv@spacecenter.dk).

Received 16 February 2006
Accepted 17 August 2006

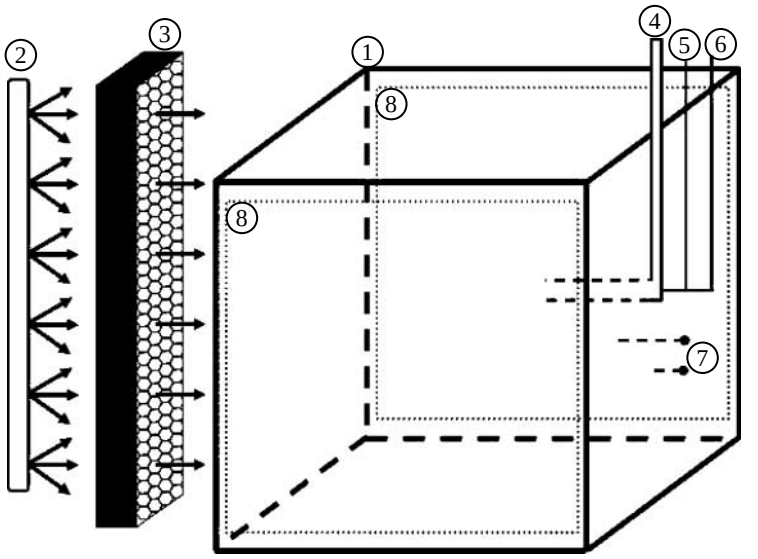

Figure 1. The reaction chamber. 1, the chamber; 2, UV array; 3, honeycomb collimator; 4, air inlet; 5, ozone line; 6, SO_2 line; 7, gas and aerosol outlet; 8, electrodes.

are active in continuously generating a reservoir of small thermodynamically stable clusters that can then rapidly grow in the presence of condensable vapours. These results demonstrate that ions probably play an important role in the production of new aerosol particles in the Earth's atmosphere.

2. Experimental procedure

The measurements were performed in a 7 m^3 reaction chamber, which was continuously flushed with purified air at 30.5 l min^{-1} at standard temperature and pressure (STP). Variable concentrations of water vapour (H_2O), ozone (O_3) and sulphur dioxide (SO_2) could be added to the chamber, which is shown schematically in figure 1. Five walls of the chamber were constructed from mylar with the final wall constructed from Teflon to allow for the transmission of UV light. Air was obtained via an inlet situated externally to the building housing the experiment. The air was compressed and dried with an oil-free compressor and then passed through a series of filters, including active charcoal, a molecular sieve, citric acid and both 10 and 3 nm particle filters. The air finally entered the experiment via a tube inserted about half a meter into the chamber.

H_2O was introduced by circulating deionized water through a GoreTex tube inserted into the air flow, which allowed the relative humidity to vary over the range 2–90%. SO_2 was added as a 5 p.p.m. mixture of SO_2 in dry air (Air Liquide) and O_3 was introduced by directing a fraction of the flow (0.5 l min^{-1} STP) through an ozone generator. Both the flows containing SO_2 and O_3 were passed through the 3 nm particle filters before mixing with the main air flow at the entrance to the chamber. At all times during the experiments, the concentrations of H_2O, SO_2 and O_3 were maintained at constant levels. Teflon tubing was used everywhere, except for a stainless steel section between the

compressor and the chamber's gas system. The pressure in the chamber was held a few Pascals above the atmospheric pressure and a stable room temperature was maintained by the laboratory air-conditioning system (296 ± 1 K). All flow outlets, used for measurements of particles and gases extended into the chamber to avoid possible artefacts from wall effects.

UV radiation, primarily at 253.7 nm, was provided by an array of seven mercury discharge lamps mounted so that they illuminated the chamber through the wall constructed from Teflon. The radiation was collimated via an 80 mm thick, honeycomb wall (1/4 in. pore size) mounted outside the chamber and coated with an UV-resistant matt black paint. The UV initiates a photochemical reaction where O_3 is photolysed to produce OH-radicals and through a series of reactions, involving SO_2, O_2 and H_2O, produces sulphuric acid (H_2SO_4). The resulting H_2SO_4 concentration was estimated using the empirical relation between aerosol growth rate and sulphuric acid concentration given by Kulmala *et al.* (2001). The UV intensity was mapped out over approximately a quarter of the chamber with a total of *ca* 21 000 measurement points across the front, middle and back of the chamber with 1 cm resolution. This ensured that the UV field was homogeneous.

Temperature, pressure and relative humidity were measured at the front wall of the chamber, the main inlet and the humidifier. Temperature was additionally measured at the top and bottom mid-points of the chamber. The O_3 and SO_2 concentrations were monitored using trace gas analysers, which were sensitive down to 0.1 p.p.b. for O_3 (Teledyne model 400A) and 0.05 p.p.b. for SO_2 (Thermo model 43 CTL). The rough composition of the gas mixture in the chamber could also be analysed using a Pfeiffer Quadrupole QMG 422 mass spectrometer.

The ions were produced in the chamber by the naturally occurring galactic cosmic radiation and the decay of the natural abundance of radon (monitored with a Durridge RAD7 instrument). In addition to this, the average production of ions could be enhanced to ionization levels relevant for the atmosphere (1–60 ion pairs $\mathrm{cm}^{-3}\,\mathrm{s}^{-1}$), with two 35 MBq Cs-137 gamma sources, placed on either side of the chamber at a distance that ensured the entire chamber was irradiated with the additional ionization. It was also possible to reduce the number of ions via an electric 'clearing' field (0–12 000 $\mathrm{V\,m}^{-1}$). This was achieved by applying a voltage drop across two acid proof stainless steel plates ($1.7 \times 1.7\ \mathrm{m}^2$) mounted within the chamber on the opposing walls. The field strength could be varied over a range of voltages corresponding to ion lifetimes of *ca* 1–200 s.

The ion current in the chamber was monitored using a Gerdien (Gerdien 1905; Aplin & Harrison 2000) type ion detector mounted on the front wall of the chamber. The detector consists of a cylindrical aluminium tube of length 25.8 cm and inner radius 1.25 cm (outer electrode), with a coaxial thin metal rod suspended at its centre (inner electrode). Air from the chamber flowed through the tube at a rate of *ca* $9\,\mathrm{l\,min}^{-1}$. By applying a positive (negative) potential across the electrodes, negative (positive) ions were forced to move towards the central electrode causing a current to flow. This current was measured by a Keithley Model 6514 electrometer. No significant difference was found between the total concentrations of positive and negative ions with mobilities greater than $1\ \mathrm{cm}^2\,\mathrm{V}^{-1}$ per second.

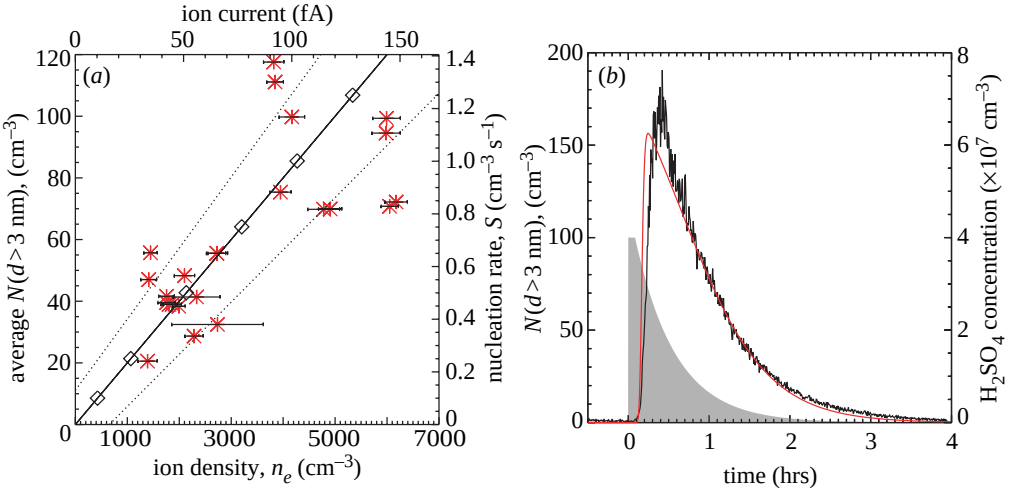

Figure 2. (*a*) $N(d>3$ nm) averaged over the 4 h cycle of each burst experiment versus ion density, n_e (red stars). The observed ion current, I, is indicated on the upper horizontal scale. The model response for a range of nucleation rates, S (black diamonds, right-hand scale), together with 1 sigma uncertainties (dotted) are also included. (*b*) A typical 4 h cycle, where $t=0$ is the time when the UV lights were activated. Plotted are the 4 h averages of $N(d>3$ nm), from both experiment (black) and model (red) with parameters (see text) $S=0.44$ cm^{-3} s^{-1}, loss term $\lambda=55\times10^{-4}$ s^{-1} and $k_0=5$. The grey shading indicates the evolution of H_2SO_4 which reaches a maximum of 4×10^7 cm^{-3} before decaying.

Varying the field strength within the tube controls, the minimum mobility of the ions contributing to the measured current and thus a spectrum of ion mobilities can be obtained. The spectra, obtained over the full range of experimental conditions reported here, indicate that the majority of small ions possess a mobility, $\mu\sim1$ cm^2 V^{-1} per second. The small ion density in the reaction chamber was then estimated from the current, I, that was measured when the potential across the electrodes was fixed at 1.23 V. This limits the small ions collected to those having a minimum mobility of approximately 1 cm^2 V^{-1} per second. The mobility cut-off is not sharply defined since ions with lower mobilities will still be collected on the central electrode if they enter the Gerdien tube near this electrode. The contribution of these ions to the current measurement can, however, be estimated from the instrument response function. Using the results from Tammet (1995), the minimum ion mobility was then converted into a maximum ion diameter of approximately 1 nm. Finally, the ion density, n_e, was obtained from $n_e(\mu>1$ cm^2 V^{-1} per second$)=I/(e\times f)$, where e is the charge per ion and f is the rate of flow through the tube. A result of this procedure is that larger ions or ionized aerosols potentially contribute to the extracted ion density, but the mobility spectra suggest that their contribution is negligible.

The number of aerosols present in the chamber was measured with a TSI Ultra Fine Condensation Particle Counter (model 3025A) capable of measuring particles in the range of 3–150 nm.

The gas mixture in the reaction chamber during all of the experiments resembles those found in the lower troposphere over the oceans, i.e. O_3 (approx.

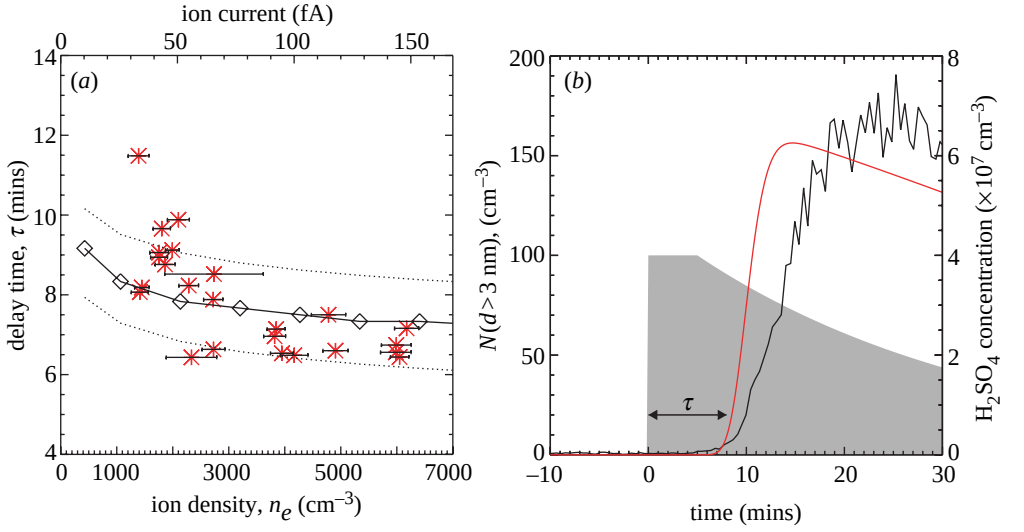

Figure 3. (*a*) Delay time, τ, as a function of ion density, n_e. (*b*) Magnification of figure 2*b* (see figure 2 caption for details).

25 p.p.b.), H_2O (approx. 35% relative humidity) and SO_2 (80–230 p.p.t.) (Seinfeld & Pandis 1998, p. 61 & 96).

3. Burst and steady-state experiments

Two types of experiments were performed: (i) a 'burst' of H_2SO_4 was produced from a short exposure to the UV light, and (ii) steady-state conditions of H_2SO_4 were achieved under continuous exposure to the UV light.

In the burst experiment, the chamber was exposed to a 10 min illumination of UV light resulting in the rapid production of sulphuric acid that reached a peak concentration around 4×10^7 cm^{-3}. This is well below the limit of homogeneous nucleation, which is around 10^9 cm^{-3} (Seinfeld & Pandis 1998, p. 578). The peak concentration lasted for a few minutes before decaying exponentially owing to losses to the walls of the reaction chamber. Figure 2*b* shows the typical response of particles larger than 3 nm, where an initial steep rise in aerosol number to a maximum is followed by a slow decay lagging the H_2SO_4 concentration. Clearly, the system possesses some very long transients requiring typically 4 h before returning to initial conditions and allowing the cycle to be repeated with another burst of UV light. The average number of particles with diameter greater than 3 nm captured by the TSI particle counter, $N(d>3$ nm), over each 4 h cycle was found to be proportional to the small ion (with $\mu>1$ cm^2 V^{-1} per second) density in the chamber (figure 2*a*).

The aerosol response to different ion densities can also be characterized by the time it takes from the initial UV exposure until the first particles begin to appear at 3 nm (figure 3*b*). This time-interval is referred to here as the delay time, τ (figure 3*b*) and is the time it takes for the aerosol concentration greater than 3 nm to reach a threshold of 10 cm^{-3}. The observed delay times also show a

dependence on the ion density, with the lowest ion densities yielding a delay time of around 11 min, which decreases to about 6 min at higher ion densities (figure 3*b*). Relaxation to steady state under continuous exposure to UV light typically took *ca* 8 h and resulted in a constant concentration of H_2SO_4 around 2×10^8 cm^{-3}. Figure 4*a* shows the number of particles larger than 3 nm obtained under steady-state conditions as a function of the observed ion-current. The typical response of the steady state $N(d>3\,\text{nm})$ under various ionization levels in the chamber can be seen in figure 4*b*. These measurements further demonstrate that the particle production depends on the ion density.

The experimental results were tested with a mixture of argon (79%) and oxygen (21%). No significant differences were observed from those described above, which suggests that the presence of nitrogen is not crucial. This indicates that particle formation involving ions most probably occurs via negative ion chemistry, since positive ion chemistry requires the presence of nitrogen (Smith & Spanel 1996).

To exclude the possibility that the experimental results obtained were due to an impurity in the compressed air, the experiments were repeated using synthetic, dry and radon free air (Synthetic Air 5.0, Strandmøllen). No discernible differences were observed. The experiments were also performed with the purified air excluding O_3 and SO_2 alternatively. The lack of particles detected at 3 nm in both the instances showed that these trace gases were essential for the observed production, although this does not rule out that additional gases are involved in the nucleation.

4. Reducing ion lifetime with the electric field

Both the 'burst' and steady-state experiments indicate that the production of new aerosol particles is proportional to the negative ion density. At these experimental conditions, it can be concluded that ions are key to producing stable clusters. Any other mechanism which could produce particles without the involvement of ions can only have made a minor contribution to the particle production. To further investigate the time-scale to produce a charged critical cluster, an electric 'clearing' field has been used. Applying an electric field of, for example, 600 V m^{-1} reduces the small ion life time to seconds, thus decreasing the time available for the ions to participate in nucleation. However, this did not have any effect on the nucleation process, and only at much larger electric field strengths did a significant response become apparent. For field strengths up to 6000 V m^{-1}, the particle production was reduced by *ca* 20% and at larger fields up to the current maximum of 12 000 V m^{-1}, the particle production was reduced by *ca* 50%. Since, as stated earlier, ions are involved in almost all particles produced, this indicates that the characteristic time for producing a stable cluster is very short, i.e. 2 s or less. The observation also indicates that the clusters become neutralized in the same time-scale as they would otherwise have been extracted from the chamber by the electric field.

In the experimental conditions reported here, classical theory suggests that the critical cluster size is of the order of 3 nm. This is based on the parametrization in Vehkamäki *et al.* (2002) and an estimate of the mole fraction of H_2SO_4 to be 0.2 (Seinfeld & Pandis 1998, p. 527). It would be surprising if the

subcritical clusters could stabilize at just under 3 nm in less than 2 s and then take a further *ca* 10 min to grow through the 3 nm detection limit. More likely the clusters have stabilized at significantly smaller diameters and then, through coagulation, generated a distribution of thermodynamically stable clusters below the 3 nm detection limit that can rapidly grow in the presence of condensable vapours. The existence of a sub-3 nm reservoir of thermodynamically stable clusters was initially proposed by Kulmala *et al.* (2000). However, they suggested ternary nucleation as the source for the reservoir rather than ions as is proposed here.

5. Numerical simulations

To investigate the size of the critical cluster k_0 and the production rate of stable clusters S under the experimental conditions, numerical simulations of particle coagulation and condensation have been compared with the experimental results. The evolution of the cluster distribution is given by (Seinfeld & Pandis 1998, p. 682)

$$\frac{\mathrm{d}N_k}{\mathrm{d}t} = \frac{1}{2}\sum_{j=2}^{k-1} K_{j,k-j}N_jN_{k-j} - \sum_{j=1}^{\infty} K_{k,j}N_kN_j - \lambda N_k + \beta_{k-1}N_{k-1} - \beta_k N_k + S\delta_{k,k_0}. \tag{5.1}$$

Equation (5.1) describes the number density, N_k, of clusters with k sulphuric acid molecules, where the equilibrium concentration of water in each cluster is reached instantaneously. The coagulation coefficient, $K_{i,j} = \pi(R_i + R_j)^2\,(\bar{c}_i^2 + \bar{c}_j^2)^{1/2}$, where $\bar{c}_i = (8k_{\mathrm{B}}T/\pi m_i)^{1/2}$ is the mean velocity of clusters with i H_2SO_4 molecules; T, temperature; k_{B}, Boltzmann constant; and R_i, the radius of a cluster with i H_2SO_4 molecules. The rate of sticking to the walls, λ, is approximated with a constant for all clusters and given by the observed loss rate of $N(d>3\,\mathrm{nm})$ during the burst experiments. The β_k-term describes the condensation of H_2SO_4 molecules in the gas phase to the kth cluster and is given by $N_1K_{k,1}$ (Seinfeld & Pandis 1998, p. 550).

In the simulation, the resulting particle distribution after a number of hours reaches a steady state between particle losses to the walls and growth by coagulation, producing a reservoir of particles with sizes below the 3 nm experimental detection limit. Following a simulated burst of UV light, this reservoir of particles begins to grow via condensation and appear above 3 nm at the rates of 1–10 $\mathrm{cm}^{-3}\,\mathrm{s}^{-1}$. The resulting evolution of simulated particles with $d>3$ nm for a single burst experiment compares favourably with the experimental data (figures 2*b* and 3*b*). By varying the free parameters k_0 and S in the model, the cumulative number of particles with $d>3$ nm is found to be dependent on both k_0 and S (figure 5*a*), while the time delay is strongly dependent on k_0 and only weakly dependent on S (figure 5*b*). To satisfy the constraint that $\tau>6$ min, requires $k_0 \leq 10$ H_2SO_4 molecules (figure 5*b*). Limiting $k_0=5$ allows for an estimate of S which is found to be of the order 0.1–1 $\mathrm{cm}^{-3}\,\mathrm{s}^{-1}$ (figure 5*a*, and right-hand axis figure 2*a*). The simulations then reproduce a delay time similar to that observed in the experiments (figure 3*a*, black diamonds), and the averaged $N(d>3\,\mathrm{nm})$ over each 4 h cycle replicates the experimental data

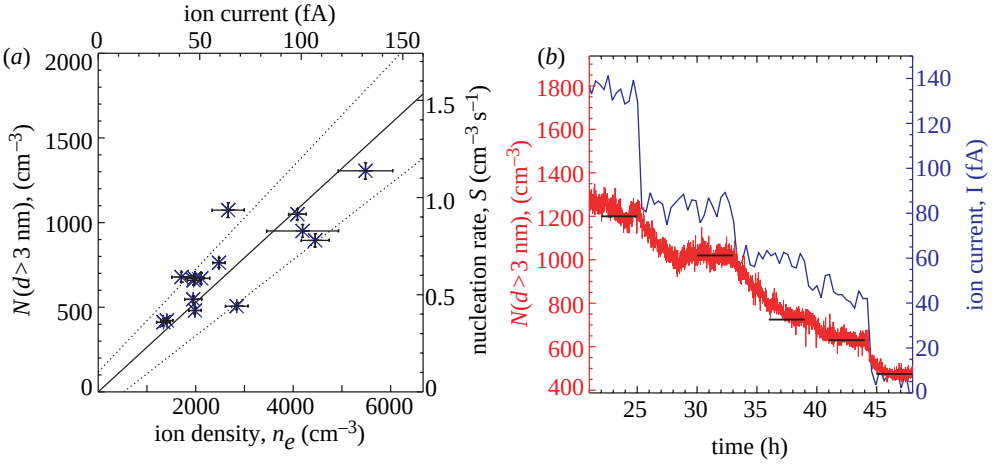

Figure 4. (*a*) $N(d>3\,\mathrm{nm})$ as a function of ion density, n_e, under steady state with environmental conditions corresponding to SO_2 (155 p.p.t.), H_2O (RH 35%) and H_2SO_4 ($2\times10^8\,\mathrm{cm}^{-3}$). The model response for a range of nucleation rates, S (black solid, right-hand scale), together with 1 sigma uncertainties (dotted) are also included. (*b*) The evolution of ion current (blue) and $N(d>3\,\mathrm{nm})$ (red) over a 2 day steady-state experiment.

very well (figure 2*a*, black diamonds). The simulations were also performed for the steady-state experiments (figure 4*a*, solid line) and these too compared favourably with the experimental data.

Recent calculations of particle production owing to ion-induced nucleation at conditions found in the lower troposphere over the oceans find much smaller production rates at 3 nm, e.g. less than 100 particles cm^{-3} in 12 h (Lovejoy *et al.* 2004). In contrast, models by Yu & Turco (2001), Yu (2006) and Laakso *et al.* (2004) indicate much higher nucleation rates in closer agreement with our results. These uncertainties in simulated nucleation rates are likely to be due to differences in the treatment of cluster thermodynamics in each model.

6. Discussion

The above experiments and simulations suggest that a mechanism is active involving ions, the trace gases SO_2, O_3 and H_2O, all at typical levels found in the atmosphere (Seinfeld & Pandis 1998, p. 61 & 96). With these gases present, the mechanism apparently produces a reservoir of stable clusters, most probably containing H_2SO_4 molecules, in the absence of UV light. The observation that the negative ion chemistry seems to be important for the nucleation process hints at the presence of an electron as necessary for stabilizing the subcritical cluster during the initial nucleation phase. To illustrate this idea, a possible pathway is presented below.

When energetic ionizing particles interact with the gas in the chamber, free electrons are produced that attach to an O_2 molecule within 10^{-9} s. The O_2^- molecule attracts a small number of water molecules, W_n, and owing to the high concentration of O_3, ligand switching with O_2 is highly probable

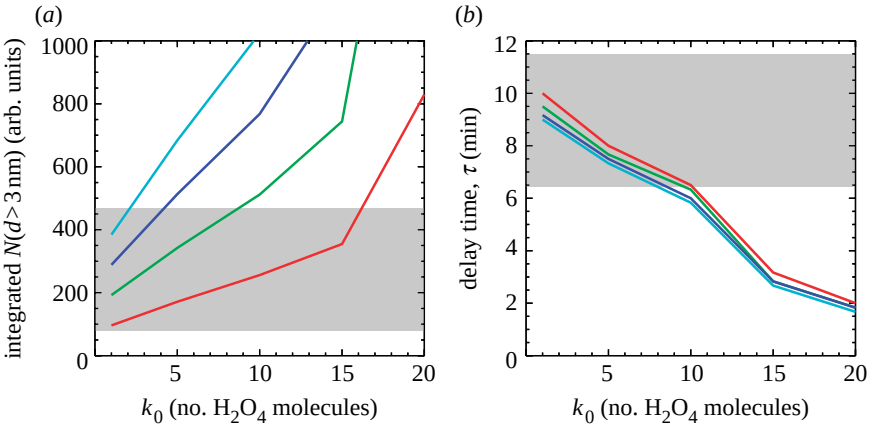

Figure 5. Numerical simulations of the burst experiment indicating how the number of H_2SO_4 molecules in a critical cluster, k_0, varies with (*a*) 4 h integrated $N(d>3\,\mathrm{nm})$ and (*b*) delay time, τ. The colours in both plots refer to the production rate S, where 0.5, 1.0, 1.5 and 2.0 $\mathrm{cm^{-3}\,s^{-1}}$ are represented by red, green, blue and light blue, respectively. Grey shading indicates the range of experimental data in figures 2 and 3.

(Fahey *et al.* 1982). This results in a negative O_3/water cluster,

$$O_2^-\cdot W_n + O_3 \rightarrow O_3^-\cdot W_{n-1} + O_2 + W_1, \tag{6.1}$$

with a reaction constant of $7\times10^{-10}\,\mathrm{cm^3\,s^{-1}}$. The above cluster initiates the oxidation of SO_2 and a corresponding charge transfer is possible (Fehsenfeld & Ferguson 1974),

$$SO_2 + O_3^-\cdot W_n \rightarrow SO_3^-\cdot W_n + O_2, \tag{6.2}$$

$$SO_2 + O_3^- \rightarrow SO_3^- + O_2, \tag{6.3}$$

where the reaction constant for reaction (6.3) is $1.7\times10^{-9}\,\mathrm{cm^3\,s^{-1}}$. If the cluster contains a sufficient number of water molecules, i.e. between 4 and 11, then SO_3^- will react with the attached water molecules and form sulphuric acid (Larson *et al.* 2000),

$$SO_3^-\cdot W_n \rightarrow H_2SO_4^-\cdot W_m. \tag{6.4}$$

The electron has now been involved in the stabilization and formation of a cluster with a single sulphuric acid molecule, however, a stable cluster has to contain several sulphuric acid molecules. The above reactions are ion reactions and the reaction constants are close to the time-scales of gas kinetic collision, thus the time-scale for generating a sulphuric acid molecule is *ca* 0.1 s for 200 p.p.t. SO_2. This process continues to form H_2SO_4 molecules with the electron acting as a catalyst and stabilizing the cluster while it is smaller than the critical size.

As indicated by the experimental results when using an electric field, the residence time of an electron in the cluster is very short, i.e. 2 s or less. The electron can become detached owing to excitation by a thermal photon or the release of chemical energy within the cluster. The detached electron might stabilize a new cluster, but there is a high probability that the electron is lost through (i) attachment to larger stable clusters, and/or (ii) recombination with a positive ion. In both the cases, the electron cannot form additional sulphuric acid

molecules. The number of stable clusters nucleated is then determined by the typical residence time of an electron in a subcritical cluster and its attachment/recombination probability once detached. The studies involving negatively charged water clusters (Beyer *et al.* 2001) suggest that the electron detachment process can take between 100 and 0.02 s. The characteristic time identified above for producing a stable cluster (2 s or less) is well within this limit, a feature not reproduced by the existing ion-induced nucleation models (Yu & Turco 2001; Laakso *et al.* 2004; Lovejoy *et al.* 2004).

Finally, it should be stressed that the presence of trace amounts of other gases in the chamber cannot be excluded. It is possible that some trace gas may not have been absorbed by the filters, and might have contributed to the nucleation process. One candidate could be NH_3 (see Kulmala *et al.* 2000). However, the presence of other condensable gases does not affect the main conclusion of this work, namely that the nucleation process under atmospheric conditions is proportional to the ion density.

The experimental data for both the burst and the steady-state experiments (figures 2*a*–4*a*) indicate that $N(d>3\,\mathrm{nm})$ is proportional to the small ion density, n_e, such that $N(d>3nm) \propto I \propto n_e$. The numerical simulations indicate that $N(d>3nm) \propto S$, which leads to the semi-empirical relation between the production rate of stable clusters, S and the ion density, n_e, viz. $S = an_e$. Under the conditions of low background aerosol, the ion density is proportional to the square root of the ion production rate, q. Note that this empirical relationship holds for both the burst and the steady-state experimental procedures. This allows for two independent estimates of the constant: for the burst experiment, $a = 2.4\times10^{-4}\pm0.4\times10^{-4}\,\mathrm{s}^{-1}$; and for the steady-state experiment, $a = 2.3\times10^{-4}\pm0.3\times10^{-4}\,\mathrm{s}^{-1}$. It is remarkable that the two different experimental procedures give the same nucleation constant. The observation that the particle production rates scale with the negative ion density suggests that it is the individual negative ions that are important, and not a collective effect between several ions, e.g. coagulation or recombination.

The experiment indicates that ions play a role in nucleating new particles in the atmosphere and that the rate of production is sensitive to the ion density. If this sensitivity is still relevant at the size of cloud condensation nuclei, one might expect to find a relationship between ionization and cloud properties (Svensmark & Friis-Christensen 1997; Svensmark 1998; Shaviv 2002). Marsh & Svensmark (2000) found that the correlation between cosmic ray ionization and clouds is mainly in low-level clouds and not as might have been expected, in high clouds where ionization variations are large.

This feature seems to be consistent with the present work. In the lower atmosphere, the limiting factor is the density of ions and, since the ion density (under conditions of low background aerosol) is proportional to $\sqrt{q}$, the sensitivity of ion density to variations in the production rate increases for decreasing values of q, i.e. $\mathrm{d}n_e/\mathrm{d}q \propto q^{-0.5}$. In contrast, at higher altitudes in the atmosphere, the ion production rate can be 10 times larger than at the surface. In these regions, it has been suggested that the role of ions saturates and the nucleation process is no longer sensitive to changes in ionization (Yu & Turco 2001). A response limited to regions where low-level clouds form is perhaps not surprising, especially when considering that high clouds usually consist of ice-particles, which involve nucleation processes not covered by the present work.

In summary, the present work indicates that (i) stable clusters are formed from SO_2, O_3 and H_2O in the presence of ions, (ii) the experiments and simulations suggest that an initial distribution of sub-3 nm stable clusters is formed containing H_2SO_4, (iii) the nucleation rate is proportional to the ion density, (iv) the negative ions are important, (v) the characteristic time for producing a stable cluster is very short 2 s or less, and (vi) the charge (electron) only stays on the small cluster for a short time 2 s or less.

References

Aplin, K. L. & Harrison, R. G. 2000 A computer-controlled Gerdien atmospheric ion counter. *Rev. Sci. Instrum.* **71**, 3037–3041. (doi:10.1063/1.1305511)

Arnold, F. 1980 Multi-ion complexes in the stratosphere—implications for trace gases and aerosol. *Nature* **284**, 610. (doi:10.1038/284610a0)

Berndt, T., Boge, O., Stratmann, F., Heintzenberg, J. & Kulmala, M. 2005 Rapid formation of sulfuric acid particles at near-atmospheric conditions. *Science* **307**, 698–700. (doi:10.1126/science.1104054)

Beyer, M. K., Fox, B. S., Reinhard, B. M. & Bondybey, V. E. 2001 Wet electrons and how to dry them. *J. Chem. Phys.* **115**, 9288–9297. (doi:10.1063/1.1413982)

Birmili, W., Berresheim, H., Plass-Dülmer, C., Elste, T., Gilge, S., Wiedensohler, A. & Uhrner, U. 2003 The Hohenpeissenberg aerosol formation experiment (HAFEX): a long-term study including size-resolved aerosol, H_2SO_4, OH, and monoterpenes measurements. *Atmos. Chem. Phys.* **3**, 361–376.

Bricard, J., Billard, F. & Madelain, G. 1968 Formation and evolution of nuclei of condensation that appear in air intially free of aerosols. *J. Geophys. Res.*, 4487.

Clarke, A. D. *et al.* 1998 Particle nucleation in the tropical boundary layer and its coupling to marine sulfur sources. *Science* **282**, 89–92. (doi:10.1126/science.282.5386.89)

Fahey, D. W., Bohringer, H., Fehsenfeld, F. C. & Ferguson, E. E. 1982 Reaction rate constants for $O_2\,(H_2O)_n$ ions n=0 to 4, with O_3, NO, SO_2 and CO_2. *J. Chem. Phys.* **76**, 1799–1805. (doi:10.1063/1.443220)

Fehsenfeld, F. C. & Ferguson, E. E. 1974 Laboratory studies of negative ion reactions with atmospheric trace constituents. *J. Chem. Phys.* **61**, 3181–3193. (doi:10.1063/1.1682474)

Gerdien, H. 1905 Demonstration eines apparates zur absoluten messung der elektrischen leitfahigheit der luft. *Phys. Zeitung* **6**, 800–801.

Hoppel, W. A., Frick, G. M., Fitzgerald, J. & Larson, R. E. 1994 Marine boundary-layer measurements of new particle formation and the effects nonprecipitating clouds have on aerosol-size distribution. *J. Geophys. Res.* **99**, 14 443–14 459. (doi:10.1029/94JD00797)

Kim, C. S., Adachi, M., Okuyama, K. & Seinfeld, J. H. 2002 Effect of NO_2 on particle formation in SO_2/H_2O/air mixtures by ion-induced and homogeneous nucleation. *Aerosol Sci. Tech.* **36**, 941–952. (doi:10.1080/02786820290092122)

Kulmala, M., Pirjola, L. & Mäkelä, J. M. 2000 Stable sulphate clusters as a source of new atmospheric particles. *Nature* **404**, 66–69. (doi:10.1038/35003550)

Kulmala, M., Dal Maso, M., Mäkelä, J. M., Pirjola, L., Väkevä, M., Aalto, P., Miikkulainen, P., Hämeri, K. & O'Dowd, C. D. 2001 On the formation, growth and composition of nucleation mode particles. *Tellus B* **53**, 479–490. (doi:10.1034/j.1600-0889.2001.530411.x)

Kulmala, M., Vehkamäki, H., Petäjä, T., Dal Maso, M., Lauri, A., Kerminen, V.-M., Birmili, W. & McMurry, P. H. 2004 Formation and growth rates of ultrafine atmospheric particles: a review of observations. *J. Aerosol. Sci.* **35**, 143–176. (doi:10.1016/j.jaerosci.2003.10.003)

Laakso, L., Anttila, T., Lehtinen, K. E. J., Aalto, P. P., Kulmala, M., Hõrrak, U., Paatero, J., Hanke, M. & Arnold, F. 2004 Kinetic nucleation and ions in boreal forest particle formation events. *Atmos. Chem. Phys.* **4**, 2353–2366.

Larson, L. J., Kuno, M. & Tao, F.-M. 2000 Hydrolysis of sulfur trioxide to form sulfuric acid in small water clusters. *J. Chem. Phys.* **112**, 8830–8838. (doi:10.1063/1.481532)

Lee, S. H., Reeves, J. M., Wilson, J. C., Hunton, D. E., Viggiano, A. A., Miller, T. M., Ballenthin, J. O. & Lait, L. R. 2003 Particle formation by ion nucleation in the upper troposphere and lower stratosphere. *Science* **301**, 1886–1889. (doi:10.1126/science.1087236)

Lovejoy, E. R., Curtius, J. & Froyd, K. D. 2004 Atmospheric ion-induced nucleation of sulfuric acid and water. *J. Geophys. Res.* **109**, D08204. (doi:10.1029/2003JD004460)

Marsh, N. D. & Svensmark, H. 2000 Low cloud properties influenced by cosmic rays. *Phys. Rev. Lett.* **85**, 5004–5007. (doi:10.1103/PhysRevLett.85.5004)

Nagato, K., Kim, C. S., Adachi, M. & Okuyama, K. 2005 An experimental study of ion-induced nucleation using a drift tube ion, mobility spectrometer/mass spectrometer and a cluster-differential mobility analyzer/Faraday cup electrometer. *J. Aerosol Sci.* **36**, 1036–1049. (doi:10.1016/j.jaerosci.2004.12.006)

Raes, F., Janssens, A. & van Dingenen, R. 1986 The role of ion-induced aerosol formation in the lower atmosphere. *J. Aerosol Sci.* **17**, 466–470. (doi:10.1016/0021-8502(86)90135-7)

Seinfeld, J. H. & Pandis, S. N. 1998 *Atmospheric chemistry and physics*. New York, NY: Wiley.

Shaviv, N. 2002 Cosmic ray diffusion from the galactic spiral arms, iron meteorites, and a possible climatic connection. *Phys. Rev. Lett.* **89**, 051102. (doi:10.1103/PhysRevLett.89.051102)

Smith, D. & Spanel, P. 1996 Ions in the terrestrial atmosphere and in interstellar clouds. *Mass Spectr. Rev.* **14**, 255–278. (doi:10.1002/mas.1280140403)

Svensmark, H. 1998 Influence of cosmic rays on Earth's climate. *Phys. Rev. Lett.* **81**, 5027–5030. (doi:10.1103/PhysRevLett.81.5027)

Svensmark, H. & Friis-Christensen, E. 1997 Variation of cosmic ray flux and global cloud coverage—a missing link in solar–climate relationships. *J. Atmos. Sol. Terr. Phys.* **59**, 1225–1232. (doi:10.1016/S1364-6826(97)00001-1)

Tammet, H. 1995 Size and mobility of nanometer particles, clusters and ions. *J. Aerosol Sci.* **26**, 459–475. (doi:10.1016/0021-8502(94)00121-E)

Turco, R. P., Zhao, J. X. & Yu, F. 1998 A new source of tropospheric aerosols: ion–ion recombination. *Geophys. Res. Lett.* **25**, 635–638. (doi:10.1029/98GL00253)

Vehkamäki, H., Kulmala, M., Napari, I., Lehtinen, K. E. J., Timmreck, C., Noppel, M. & Laaksonen, A. 2002 An improved parameterization for sulfuric acid–water nucleation rates for tropospheric and stratospheric conditions. *J. Geophys. Res.* **107**, 4622. (doi:10.1029/2002JD002184)

Vohra, K. G., Ramu, M. C. S. & Muraleedharan, T. S. 1984 An experimental-study of the role of radon and its daughter products in the conversion of sulfur-dioxide into aerosol-particles in the atmosphere. *Atmos. Environ.* **18**, 1653–1656. (doi:10.1016/0004-6981(84)90387-1)

Wilhelm, S., Eichkorn, S., Wiedner, D., Pirjola, L. & Arnold, F. 2003 Ion-induced aerosol formation: new insights from laboratory measurements of mixed cluster ions $HSO_4^-(H_2SO_4)(a)(H_2O)(w)$ and $H^+(H_2SO_4)(a)(H_2O)(w)$. *Atmos. Environ.* **38**, 1734–1744.

Yu, F. & Turco, R. P. 2001 From molecular clusters to nanoparticles: role of ambient ionization in tropospheric aerosol formation. *J. Geophys. Res.* **106**, 4797–4814. (doi:10.1029/2000JD900539)

Yu, F. 2006 From molecular clusters to nanoparticles: second-generation ion-mediated nucleation model. *Atmos. Chem. Phys. Discuss.* **6**, 3049–3092.